Available online at www.sciencedirect.com
SCIENCE DIRECT®
Surface Science 526 (2003) 107–114
SURFACE SCIENCE
www.elsevier.com/locate/susc

$SrTiO_3(0\,0\,1)$ surface structures under oxidizing conditions

N. Erdman *, L.D. Marks *

Department of Materials Science and Engineering, Institute for Environmental Catalysis, Northwestern University, 2220 Campus Dr., Evanston, IL 60208-3108, USA

Received 16 October 2002; accepted for publication 21 November 2002

Abstract

The thermodynamically stable (2×1), $c(4 \times 2)$ and $c(6 \times 2)$ surface structures were obtained under oxidative conditions on the $SrTiO_3(0\,0\,1)$ surface and studied with transmission electron microscopy. All three reconstructed surfaces exhibit similar morphological features—formation of flat $\langle 1\,0\,0 \rangle$ facets on the surface, stabilization of $\langle 1\,1\,0 \rangle$ originally polar facets as well as the existence of surface defects in a form of subsurface voids. The consistency and high reproducibility of our results suggest construction of a phase diagram for the formation of different structures on the $SrTiO_3(0\,0\,1)$ surface as a function of annealing temperature.
© 2002 Elsevier Science B.V. All rights reserved.

Keywords: Surface relaxation and reconstruction; Faceting; Surface structure, morphology, roughness, and topography; Single crystal surfaces; Surface defects

1. Introduction

Oxide surfaces are important scientifically as well as technologically for application in catalysis and thin film growth. $SrTiO_3$ is considered a standard model for oxides with a perovskite structure—a close-packed lattice of oxygen and strontium in a 3:1 ratio, with titanium in octahedral interstitial sites. It has been used as a substrate for epitaxial growth of superconducting thin films [1,2] and a buffer layer for the growth of GaAs thin films on Si [3]. For an ideal, bulk-terminated $(0\,0\,1)$ surface, two configurations are possible: (a) Ti and O termination with a ratio of 1:2 (TiO_2 stoichiometry); or (b) Sr and O termination with a ratio of 1:1 (essentially SrO). However, since the valence and coordination numbers of transition metal oxides typically depend on environmental conditions (atmosphere, pressure and temperature), the picture becomes rather complicated. A large number of studies in recent years have used numerous surface science techniques in an effort to understand surface structure variations in $SrTiO_3(0\,0\,1)$ under different experimental conditions [4–14]. A summary of the literature results is presented in Table 1.

The results obtained by different groups are sometimes contradictory, and only a few of the studies have attempted to support their results with a feasible model for the surface structures. Cord and Courths [4] investigated $SrTiO_3$ surfaces

* Corresponding authors. Tel.: +1-847-391-2028; fax: +1-847-391-7820 (N. Erdman). Tel.: +1-847-491-3996 (L.D. Marks).
E-mail addresses: nerdman@uop.com (N. Erdman), l-marks@nwu.edu (L.D. Marks).

0039-6028/02/$ - see front matter © 2002 Elsevier Science B.V. All rights reserved.
PII: S0039-6028(02)02573-6

Table 1
Summary of the results obtained by different groups on $SrTiO_3(0\,0\,1)$ surface structures

Observed reconstruction	Sample preparation	Technique
(1×1)	(1) UHV annealing, $T = 1100$ K, 60 min [4–8] (2) Annealing in 10^{-5} mbar O_2 [4,5]	AES [4,8], LEED [4–8], AFM [5], STM [6], UPS [5], RHEED [5], MEIS [5]
(2×1)	(1) Annealing in 10^{-5} mbar O [4] (2) UHV annealing, $T = 950$ °C, 2 h [8] (3) UHV annealing, $T = 600$–800 °C, 30 min [8,10]	LEED, AES, STM [8,10]
(2×2)	Annealing in 10^{-5} mbar O_2 [4,5]	LEED [4], MEIS [5], AES [4], RHEED [5], UPS [5]
$c(4 \times 2)$	UHV annealing in 10^{-5} mbar H_2, $T = 950$ °C, 2 h [8,10,13]	LEED, AES, STM
$c(6 \times 2)$	O_2 annealing, $T = 1100$ °C, 3 h; followed by UHV annealing, $T = 950$ °C, 2 h [8,10,12]	LEED [8,10,12], AES [8], STM [8,10,12]
(6×2)	O_2 annealing, $T = 1100$ °C, 3 h; followed by UHV annealing, $T = 950$ °C, 2 h [11]	LEED, STM
$(\sqrt{5} \times \sqrt{5})R26.6°$	(1) UHV annealing, $T = 900$ °C, 15h; then flashing at $T = 1200$ °C, 2 min [13] (2) UHV annealing, $T = 830$ °C, 120 min [14]	RHEED [13], XPS [13,14], STM [13,14], LEED [13,14]

annealed in UHV and oxygen atmosphere by photoemission spectroscopy, low-energy electron diffraction (LEED) and Auger spectroscopy (AES). The oxygen annealed structures determined by LEED ((2×1) and (2×2)) were thermodynamically stable and stoichiometric; their electronic stability was attributed to formation of the Ti^{+3}–O vacancy complexes on the surface, in effect creating a TiO_x-rich surface. In STM and AFM studies, Liang and Bonnell [6,7] observed that upon UHV annealing, a rearrangement of surface atoms resulted in the formation of row-like structures with spacings of 12 and 20 Å. The authors proposed two structural reorganization mechanisms: (a) the formation of new phases on the surface upon reduction, accompanied by changes in the composition and geometry of the surface; and (b) an alteration of the surface morphology due to a reordering of oxygen vacancies. Based upon the observed spacings they attributed the observed surface to an SrO-rich surface with the formation of the so-called Ruddlesden–Popper phases [15]. This conclusion was based on an assumption of different sublimation rates for Sr, Ti and O at the surface, i.e. TiO_x has a higher sublimation rate than SrO at high temperatures in vacuum. A more recent AFM study by Szot et al. [16] suggested that oxidation above 900 °C can also cause the $SrTiO_3(0\,0\,1)$ surface to become SrO-rich, albeit without chemically characterizing the surface. These conclusions were based on measurements of step heights (consistent with unit cell dimensions of several Ruddlesden–Popper phases) from AFM images. The authors proposed that under oxidizing conditions at high temperatures, the near-surface region reconstructs via dismantling, transport and intercalation of SrO layers combined with a crystallographic shearing mechanism.

Other studies suggest that the vacuum annealed surface is depleted in SrO and is primarily covered by TiO_2 planes [10,13]. Jiang and Zegenahgen [8,12] used STM and LEED to observe a well-ordered and atomically flat surface after annealing in vacuum at different temperatures. Further observations showed the existence of domains rotated by 90° with respect to one-another as well as the formation of single unit cell high steps on the surface. In the same experiment a change in Auger peak intensity ratios (O-to-Ti and Sr-to-Ti) was observed for the (2×1), $c(4 \times 2)$ and $c(6 \times 2)$ surface structures. The Auger spectroscopy results suggested that the reconstructions with larger size unit cells tends to be richer in Ti. Formation of

$Sr_{n-1}Ti_nO_{3n-1}$-type phases on the surface was suggested as a possible explanation of the features and periodicities obtained in STM images [8,12]. The authors also proposed that two competing processes—bulk oxygen diffusion and oxygen desorption from the surface—determine the final structure of the surface.

Castell [10,11] used chemical etching and/or argon ion sputtering and subsequent UHV annealing to obtain (2×1), $c(4 \times 2)$ and (6×2) structures on the $SrTiO_3(0\,0\,1)$ surface. The surface, inspected by LEED and STM, showed large surface steps with 0.4 nm step height. The author proposed structural models based on a qualitative interpretation of the STM images, in particular step height measurements and periodicities of the surface features. The models for different structures are simple modifications of the bulk-like TiO_2-terminated surface: for each of the models the author proposed a removal of one or several rows of Ti atoms to match the periodicity observed in the STM images, in fact creating variations in surface stoichiometry (e.g. Ti_2O_3 for the (2×1) surface, TiO_2 for the $c(4 \times 2)$ surface). No surface chemical probes were reported that provide definitive evidence for such titanium enrichment. Castell [10,11] rejected the idea that impurity segregation is a governing factor in the formation of various $SrTiO_3$ surface structures.

Alongside the numerous experimental studies, a few researchers have presented theoretical calculations for the $SrTiO_3(0\,0\,1)$ surface, mainly addressing the issues of surface electronic band structure and surface relaxation [17–19]. Ab-initio calculations using the shell model [17] showed that the surface energies of bulk-like Sr-terminated and Ti-terminated (0 0 1) surfaces are nearly equal, implying that the two types of surfaces can coexist experimentally. It has also been suggested [18] that the surface termination essentially depends on the growth conditions, and there is a slight preference for the TiO_2 termination.

STM and AFM observations collected by several groups have provided some insight into the morphological characteristics of reconstructed $SrTiO_3$ surfaces, while LEED and various spectroscopy techniques have provided supporting crystallographic and chemical information. This being said, there has not been a comprehensive study to provide a 'recipe' for consistent and reproducible preparation of various $SrTiO_3$ surfaces.

In this paper we focus on the morphology of the thermodynamically stable (2×1), $c(4 \times 2)$ and $c(6 \times 2)$ surface structures obtained under oxidative conditions on the $SrTiO_3(0\,0\,1)$ surface and studied with transmission electron microscopy (TEM) techniques. TEM allows an almost simultaneous identification of the surface crystallography through electron diffraction as well as characterization of the morphology of a particular surface through a combination of bright/dark field imaging and high-resolution microscopy. Our study represents a comprehensive effort to obtain consistent and highly reproducible results for the various $SrTiO_3(0\,0\,1)$ surface terminations and determine the exact conditions for formation of these structures. The surface structure solutions will not be discussed further here and can be found elsewhere [20,24].

2. Experimental

Single crystal $SrTiO_3(0\,0\,1)$ wafers with dimensions $10 \times 10 \times 0.5$ mm^3 were cut using a rotary disc cutter to obtain 3mm discs, a nominal size for a TEM sample. The discs were mechanically polished to a thickness of about 100 μm. Subsequently the discs were dimpled and polished. Each sample was then ion milled with 4.8 kV Ar^+ ions using a Gatan Precision Ion Polishing System (PIPS) to produce an electron transparent sample. In order to eliminate the damage caused to the sample in the process of ion milling and achieve a reconstructed surface, the samples were annealed at atmospheric pressure in a tube furnace in a range of temperatures from 850 to 1100 °C with a constant flow of oxygen. Although the partial pressure of oxygen in these experiments was not measured precisely, it was close to partial pressure of oxygen in air. The annealing time for all the samples was 0.5–5 h. A critical point to be addressed is the cleanliness of the apparatus being used (i.e. the alumina crucible and the quartz or alumina tube). Both the crucible and the tube were cleaned prior to annealing using an *aqua regia* solution ($HCl + HNO_3$), washed thoroughly with deionized

water and dried using acetone. The carbonaceous residue left on the inside of the tube was removed by heating the apparatus at 300 °C for approximately an hour prior to use. This procedure ensured minimal contamination of the sample during the annealing.

All the surface structures appear to be exceptionally stable in air (no changes observed in the samples over a period of months). Significantly, the same sample could be used to produce different surface structure simply by reannealing in a different temperature regime, indicating that they are thermodynamically, not simply kinetically, stable. Off-zone axis electron diffraction patterns and bright/dark-field images were obtained using the UHV-H9000 Hitachi electron microscope operated at 300 kV at Northwestern University.

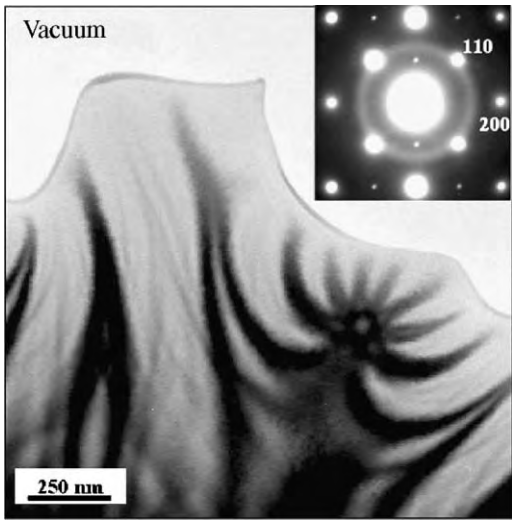

Fig. 1. Bright-field image and corresponding selected area diffraction pattern of the ion-milled $SrTiO_3(0\,0\,1)$ surface prior to annealing. The bright-field image shows strain effects such as bend contours.

3. Results

3.1. Unannealed surface

After ion-milling and prior to annealing, the surface of $SrTiO_3(0\,0\,1)$ exhibits some disorder and strain. Fig. 1 shows a bright-field image and corresponding diffraction pattern of a typical sample. The diffraction pattern has two distinct features: bulk diffraction spots as well as an amorphous ring that can be attributed to a disordered surface layer resulting from ion-milling. The bright-field image shows strain effects such as bend contours. These findings suggest that the unannealed, ion-milled surface is unreconstructed and does not exhibit an ordered (1×1) structure.

3.2. (2×1) surface

Samples annealed at a range of temperatures from 950 to 1030 °C exhibited a (2×1) surface structure. Fig. 2 shows a bright-field image of the $SrTiO_3(0\,0\,1)$ sample combined with an off-zone axis selected area diffraction pattern. Reflections from both 2×1 and 1×2 domains are present. The diffraction spots can be characterized as follows: (a) strong bulk diffraction spots; (b) weaker bulk spots (present due to the difference in structure factors of Sr and Ti); and (c) relatively weak surface reflections. The bright-field image shows rapid thickness variation of the sample towards the edge, obvious from the dark/bright contrast

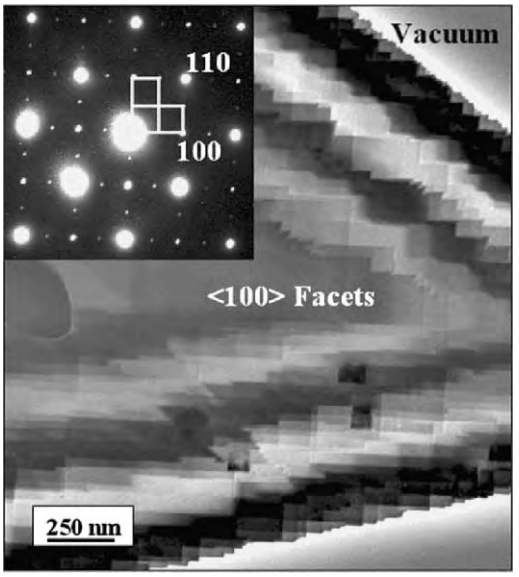

Fig. 2. Bright-field image and corresponding off-zone axis diffraction pattern of the (2×1) $SrTiO_3(0\,0\,1)$ surface formed after annealing at 950–1050 °C. The surface unit cell for both domains of the reconstruction is marked.

change of thickness fringes. This image indicates the formation of large flat $\langle 1\,0\,0\rangle$ facets on the surface of the sample due to annealing. Formation of similar atomically flat terraces was observed in several previous AFM and STM studies [8,12,16].

3.3. $c(4 \times 2)$ surface

Samples annealed at lower temperature regime (830–930 °C) exhibit a $c(4 \times 2)$ surface structure. An example of a typical $c(4 \times 2)$ off-zone axis diffraction pattern as well as a high-resolution bright-field image is presented in Fig. 3. The image shows several different morphological features-large surface steps (50–200 nm wide) as well as rectangular features ~2–10 nm in size. Whereas the majority of the step edges are oriented along [1 0 0] or [0 1 0] directions, in some areas it can be clearly seen that $\langle 1\,1\,0\rangle$ type facets are stabilized as well as a result of annealing.

3.4. $c(6 \times 2)$ surface

Higher temperatures (1050–1100 °C) were used to prepare a $c(6 \times 2)$ surface structure. Fig. 4 shows a dark-field image obtained from the $c(6 \times 2)$ surface using a (1 1 0) reflection and the inset shows an off-zone axis diffraction pattern from the same surface.The image clearly shows formation of a domain structure, with two variants at 90°. The general morphology of the surface is similar to the other $SrTiO_3(0\,0\,1)$ reconstructed surfaces described above.

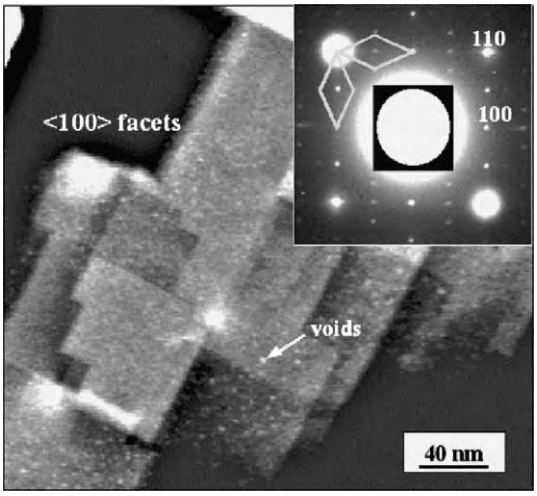

Fig. 3. Bright-field image and corresponding diffraction pattern of the $c(4 \times 2)$ $SrTiO_3(0\,0\,1)$ surface formed after annealing at 850–930 °C. The primitive surface unit cell for both domains of the reconstruction is marked.

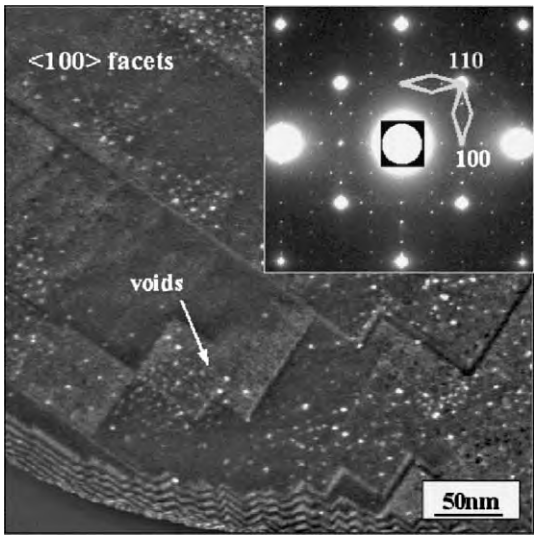

Fig. 4. Dark-field image and corresponding diffraction pattern of the $c(6 \times 2)$ $SrTiO_3(0\,0\,1)$ surface formed after annealing at 1050–1100 °C. The primitive surface unit cell for both domains of the reconstruction is marked.

3.5. Voids

The small rectangular features that can be clearly seen in Figs. 3 and 4 are attributed to voids. The features show no strain contrast, suggesting that they are neither precipitates nor trapped gas bubbles. They are clearly located in the near-surface region of the sample; if the voids were extremely deep then their density would increase as the sample thickness becomes greater, but this was not observed. It is important to note that the voids are unrelated to the reconstruction itself: the steps and surface domains can be seen crossing the voids unperturbed. The number of voids observed per sample area was governed mainly by the sample preparation procedure (i.e. the amount of ion

milling prior to annealing, as well as the annealing temperature and time). Similar features, though larger in dimensions (~20–50 nm in length and width, 12 Å deep) were observed by Jiang et al. [8] and were attributed to holes in the sample due to thermal etching.

Multislice simulations were performed in order to verify that the contrast of these rectangular features seen in HREM images corresponds to voids and is not due to a precipitate of a different phase or a hole on the sample surface. For the purposes of the simulation, a 10×10 unit cell (39.05×39.05 Å^2) slab of $SrTiO_3$ with a total thickness of 200–250 Å was used. The shape of the void was assumed to be a rectangular parallelepiped positioned in the middle of the slab. The dimensions of the void were 5×5 unit cells in projection (19.525×19.525 Å^2). The parameters varied during the calculation were the relative position of the void with respect to the surface layer (1–5 bulk unit cells) and the thickness of the void (2–5 bulk unit cells). The results of the simulations were compared to the HREM images of the voids obtained using a JEOL 4010 electron microscope at Argonne National Lab operated at 400 kV. The experimental HREM image and the multislice simulation of a void, both shown in Fig. 5, are in fairly good agreement with each other. The simulation results suggest that the void is positioned approximately 10 Å below the surface layer.

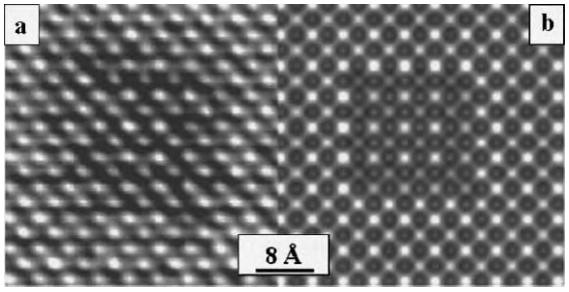

Fig. 5. (a) HREM image of the void taken using JEOL 4010 electron microscope at ANL, and (b) multislice simulation of the void (−40 nm). For this simulation the total thickness of the sample was 253.53 Å, with the void thickness of 9.76 Å. The void was positioned 10 Å below the top surface.

4. Discussion

The $SrTiO_3$ surface structures produced under oxidizing conditions described here are highly reproducible and can be obtained on the same crystal simply by changing the annealing temperature. The temperatures used in these annealing experiments are approximately 1/3 to 1/2 of the melting temperature of $SrTiO_3$, assuring a significant amount of surface diffusion capable of producing well-ordered, faceted surfaces. Faceting, therefore, can be considered a strong indication that the surface has equilibrated. Longer annealing times produce larger facets and reduce the number and size of the surface defects.

The fact that the majority of the step edges are oriented along the [1 0 0] and/or [0 1 0] directions, the sharpness of the facet edges, and the rectangular shape of the voids all suggest that the {1 0 0} facets are the most stable surfaces. On the other hand, an interesting feature common to all of the reconstructions is the formation of ⟨1 1 0⟩ facets in some areas of the samples. The unreconstructed $SrTiO_3$(1 1 0) surface is polar—in this case the repeat unit contains alternating layers of SrTiO (net charge of +4) and O_2 (net charge −4). The layers are unquestionably charged, therefore creating a net dipole moment. Brunen et al. [21] investigated the (1 1 0) surface of $SrTiO_3$ under a variety of annealing conditions using LEED, AFM and STM. Their results showed the formation of a large number of reconstructions of the type $(n \times m)$; moreover, LEED and STM data suggested that some of these structures are incommensurate with the underlying bulk lattice. Our preliminary results from TEM analysis of $SrTiO_3$(1 1 0) samples also suggest that the (1 1 0) surface does reconstruct upon annealing the sample at 900 °C (Fig. 6). Some of the morphological features we observed on the reconstructed (1 1 0) surface are similar to those found on the (1 0 0) surface—formation of large facets as well as rectangular shaped surface defects. The diffraction pattern in Fig. 6 shows the presence of surface reconstruction, and the corresponding dark-field image shows a formation of a row-like structure that has formed along the [−1 1 0] direction on the surface. These results are consistent with the investigation of the (1 1 0) surface reported

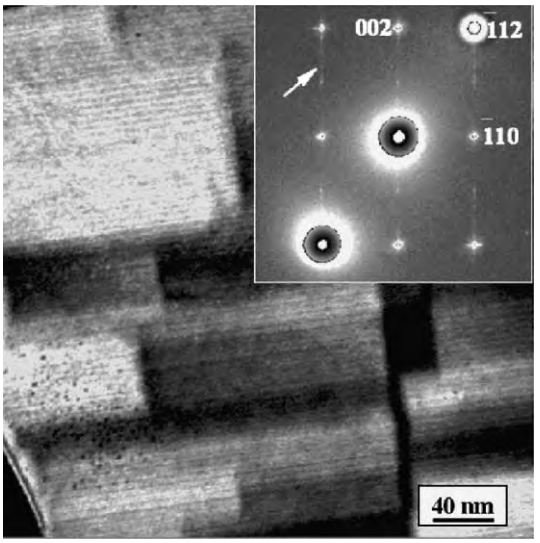

Fig. 6. Dark-field image and corresponding diffraction pattern of the reconstructed $SrTiO_3(1\,1\,0)$ surface formed after annealing at 900 °C. The arrow in the diffraction pattern is pointing to the streaks along (0 0 1) due to the reconstructed surface.

by Brunen et al. [21]. Our results are particularly interesting because they could potentially provide an insight into the reconstruction of charged oxide surfaces as a way of stabilizing such surfaces.

The type of the reconstruction produced on the $SrTiO_3$ surface is dependent more on the thermodynamics than on the kinetics of the process. Independent of the annealing time (ranging from 0.5 to 5 h), all of the reconstructions described above can be achieved on the same sample by simply changing the annealing temperatures. The amount of time necessary to reconstruct an ion-milled surface depends mainly on the degree of disorder and damage inflicted on the surface due to the sputtering process—i.e., increasing the amount of time spent ion-milling a sample consequently increases the length of time necessary to recover the surface. Another experimental aspect to be taken into consideration is the effect of thermal etching on surface stoichiometry. Thermal etching of $SrTiO_3$ surfaces at elevated temperatures was studied extensively by Tomashpolskii et al. [22,23], and their findings suggest that depending on the temperature, SrO or TiO_2 is preferentially removed from the surface. In the range of the temperatures described here, the SrO evaporation is more likely (supported also by the XPS and UPS data from other groups, e.g. [5,19]). This process results in the essentially TiO_2 stoichiometry that we have observed for the (2×1) and the $c(4 \times 2)$ surfaces [20,24]. Therefore, it is clear that the original unreconstructed (0 0 1) surface is extremely unstable at high temperatures, and it rearranges itself through a large amount of mass-transfer as well as surface reconstruction. Note that the experiments described here were conducted only under oxidizing environments; therefore the effect of oxygen partial pressure on this system is yet to be determined. It is unclear at this stage whether the reconstructions with similar dimensions observed under UHV conditions by other groups (see Table 1) are structurally identical to the ones obtained by our group or, or if certain pairs of UHV-annealed and oxidized surfaces just share the same unit cell periodicity, although we strongly doubt this.

The consistency and reproducibility of the above results, and most importantly the fact that the above structures can be obtained on the same sample just by changing the temperature of the experiment, suggest that a $SrTiO_3(0\,0\,1)$ surface phase diagram may be readily constructed. Deciding which two variables to use is a little difficult. While temperature must certainly be one variable, both surface stoichiometry and oxygen partial pressure could be considered plausible candidates for the second parameter. Currently, we have identified the stoichiometry of the (2×1) and the $c(4 \times 2)$ surfaces (in both cases TiO_2), but are not completely sure about that of the $c(6 \times 2)$ surface. Thus, it would be difficult to construct a phase diagram using compositional variations. However, we know that the above structures can be obtained both in air and in a flow of oxygen, suggesting that there is a dependence, albeit quite weak, of the obtained structure on the partial pressure of oxygen under oxidizing conditions. Based on these observations and information from Ellingham diagrams of binary and ternary oxides, we propose the partial surface phase diagram for $SrTiO_3$ shown in Fig. 7. The $c(4 \times 2)$ structure is the most stable of the three structures and forms at low

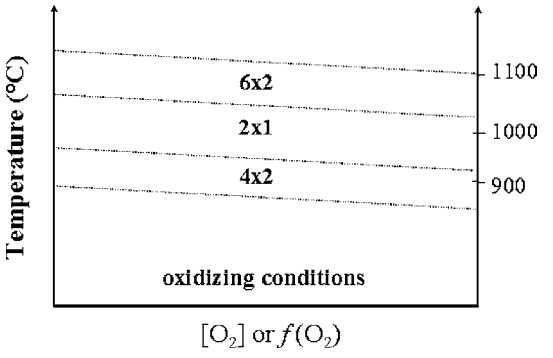

Fig. 7. Partial surface phase diagram for formation of different structures on $SrTiO_3(0\,0\,1)$ surface as a function of annealing temperature.

temperatures, whereas the c(6 × 2) surface is the least stable. Further investigation is required to fully understand the influence of oxygen partial pressure on the system.

5. Conclusions

We have investigated the thermodynamically stable (2 × 1), c(4 × 2) and c(6 × 2) reconstructions on the $SrTiO_3(0\,0\,1)$ surface obtained under oxidative conditions using TEM. All three reconstructed surfaces exhibit similar morphological features—formation of flat $\langle 1\,0\,0\rangle$ facets on the surface, stabilization of $\langle 1\,1\,0\rangle$ originally polar facets as well as the existence of surface defects in a form of subsurface voids. The formation of the observed reconstructions is temperature dependent: the c(4 × 2) structure forms at low temperatures (830–930 °C), the (2 × 1) structure forms at 950–1030 °C and the c(6 × 2) structure forms at high temperatures (1050–1100 °C). Based on our results, we have proposed a partial phase diagram for the formation of different structures on the $SrTiO_3(0\,0\,1)$ surface as a function of annealing temperature, though the effect of oxygen partial pressure on this system is yet to be fully understood.

Acknowledgements

This work was supported by the EMSI program of the National Science Foundation and the US Department of Energy Office of Science (CHE-9810378) at the Northwestern University Institute for Environmental Catalysis. HREM analysis was carried out at the Electron Microscopy Collaborative Research Center at Argonne National Laboratory.

References

[1] C. Aruta, Phys. Status Solidi A 183 (2001) 353.
[2] P. Chaudhari, R.H. Koch, R.B. Laibowitz, T.R. McGuire, R.J. Gambino, Phys. Rev. Lett. 58 (1987) 2687.
[3] R. Droopad, Z. Yu, J. Ramdani, L. Hilt, J. Curless, C. Overgaard, J. Edwards Jr., J. Finder, K. Eisenbeiser, W. Ooms, Mater. Sci. Eng. B 87 (2001) 292.
[4] B. Cord, R. Courths, Surf. Sci. 162 (1985) 34.
[5] T. Nishimura, A. Ikeda, H. Namba, T. Morishita, Y. Kido, Surf. Sci. 421 (1999) 273.
[6] Y. Liang, D.A. Bonnell, Surf. Sci. Lett. 285 (1993) L510.
[7] Y. Liang, D.A. Bonnell, Surf. Sci. 310 (1994) 128.
[8] Q.D. Jiang, J. Zegenhagen, Surf. Sci. 425 (1999) 343.
[9] M. Naito, H. Sato, Physica C 229 (1994) 1.
[10] M.R. Castell, Surf. Sci. 505 (2002) 1.
[11] M.R. Castell, Surf. Sci. 516 (2002) 33.
[12] Q.D. Jiang, J. Zegenhagen, Surf. Sci. Lett. 285 (1995) L882.
[13] T. Matsumoto, H. Tanaka, T. Kawai, S. Kawai, Surf. Sci. 318 (1994) 29.
[14] M.S. Martin-Gonzalez, M.H. Aguirre, E. Moran, M.A. Alario-Franco, V. Perez-Dieste, J. Avila, M.C. Asensio, Solid State Sci. 2 (2000) 519.
[15] S.N. Ruddlesden, P. Popper, Acta Crystallogr. 11 (1958) 54.
[16] K. Szot, W. Speier, Phys. Rev. B 60 (1999) 5909.
[17] E. Heifets, S. Dorfman, D. Fuks, E. Kotomin, A. Gordon, J. Phys. C 10 (1998) L347.
[18] J. Padilla, D. Vanderbilt, Surf. Sci. 418 (1998) 64.
[19] V.E. Heinrich, Prog. Surf. Sci. 44 (1983) 175.
[20] N. Erdman, K.R. Poeppelmeier, M. Asta, O. Warschkow, D.E. Ellis, L.D. Marks, Nature 419 (2002) 55.
[21] J. Brunen, J. Zegenhagen, Surf. Sci 389 (1997) 349.
[22] Y.Y. Tomashpolskii, I.Y. Kolotyrkin, E.N. Lubnin, J. Microsc. Spectrosc. Electron. 10 (1985) 521.
[23] Y.Y. Tomashpol'skii, E.N. Lubnin, M.A. Sevost'yanov, V.I. Kukuev, Sov. Phys. Crystallogr. 27 (1981) 691.
[24] N. Erdman, O. Warschkow, M. Asta, D.E. Ellis, K.R. Poeppelmeier, L.D. Marks, in preparation.